

Lamellar Thickening Growth of an Extended Chain Single Crystal of Polyethylene. 1. Pointers to a New Crystallization Mechanism of Polymers

M. Hikosaka* and K. Amano

*Faculty of Integrated Arts and Sciences, Hiroshima University,
Higashi-Hiroshima, 739 Japan*

S. Rastogi

*Laboratory of Polymer Chemistry and Technology, Technische Universiteit Eindhoven,
Eindhoven, The Netherlands*

A. Keller

H. H. Wills Physics Laboratory, University of Bristol, Bristol, BS8 1TL U.K.

*Received May 21, 1996; Revised Manuscript Received December 26, 1996**

ABSTRACT: Crystallization and growth of an isolated extended chain single crystal (ECSC) of polyethylene (PE) under high pressure from the melt into the mobile phase, such as hexagonal phase, was studied by in-situ optical microscopy and transmission electron microscopy. Direct evidence is obtained that an isolated ECSC was formed from a folded chain single crystal through the combination of newly recognized "lamellar thickening growth" and the long familiar lateral growth. This confirmed the prediction of chain sliding diffusion theory that the lamellar thickening growth takes place the important role in the origin of folded chain and extended chain crystals (FCCs and ECCs) presented by one of authors (M.H.) previously. The lamellar thickness (l) increased linearly with time (t), indicating that the lamellar thickening growth rate is constant as long as the crystal is in isolation, i.e., it does not impinge on others, directly reflected also by the straightened taper of the cross-sectional shape. This is quite different from the well-known lamellar thickening of stacked-lamellar system where l increases linearly with logarithm of time ($\log t$). It is shown that the difference is due to the difference between the primary and the secondary crystallization processes. The lamellar thickening growth rate (U), defined by $(dl/dt)/2$, was measured for the first time by developing two methods, "direct method" and "mapping method".

1. Introduction

It is well-known that polymers show two typical morphologies: folded chain crystals (FCCs) first identified by Keller¹ and extended chain crystals (ECCs) first observed by Wunderlich and Arakawa.² Here we will define FCCs and ECCs after Wunderlich: FCCs are thin lamellar crystals with thicknesses which usually range between 5 and 50 nm, whereas ECCs are thick lamellar crystals which have thicknesses of at least 0.2 μm .³

They are seen both in single crystals and in bulky solids. The physical properties of polymer solids strongly depend on these morphologies. Therefore, studies on the growth mechanism and origin of FCCs and ECCs are important for both basic polymer science and polymer technology.

It is obvious that the long known lateral growth is important in the formation of FCCs of polymers. Numerous studies have been carried out on the lateral growth of FCCs.

Lamellar thickening of stacked lamellae of FCCs in annealing or isothermal crystallization was another interesting topic, because it is one of the most important structural and morphological changes which takes a role in improving the physical properties of polymer materials. It is essentially a reorganization process of polymer chains within stacked lamellae, therefore the secondary crystallization process.

Note that secondary crystallization should be distinguished from the primary crystallization of a single crystal, because in the former case no new chains are

introduced into the lamellae, while the latter is essentially a nucleation and growth process by introducing new polymer chains from the melt or solution into the single crystal.

Many studies on the lamellar thickening were done in the 1960s by Statton and Geil,⁴ Fischer and Schmidt,⁵ Anderson,⁶ Peterlin,⁷ Hirai, and so on.⁸ They showed that the long period of the stacked lamellae (L) increased with increasing annealing temperature (T_{ann}) or crystallization temperature (T_c) and that this L increased linearly with the logarithm of time ($\log t$), that is,

$$L = W \log t + p \quad (1)$$

where W and p are constants.⁵ Peterlin found that the lamellar thickening rate (W) defined by the relation

$$W = dL/d(\log t) \quad (2)$$

increases with increasing T_c . This means that the value of W decreases with an increase in ΔT , i.e.,

$$dW/d\Delta T < 0 \quad (3)$$

As to the origin of ECCs of polyethylene (PE), Uhlmann⁹ and Takemura et al.¹⁰ maintained that ECCs are formed directly from the melt, while Wunderlich et al.¹¹ and Bassett et al.¹² insisted that ECCs are formed from FCCs through lamellar thickening. Note that they studied a stacked lamellar system, i.e., the secondary crystallization process.

* Abstract published in *Advance ACS Abstracts*, March 1, 1997.

An isolated ECC of PE was first studied by Bassett.¹³ Bassett observed by means of electron transmission microscopy an isolated ECC and first found that its cross section shows a tapered shape and suggested for the first time an important correspondence of the tapered shape to the thickening of the single lamella.¹⁴

Bassett also found that the ECC structure arises when the melt crystallizes into the hexagonal phase and the FCC structure (as long known before) into the orthorhombic phase.¹⁵ Yamamoto showed based on X-ray observation that in the hexagonal phase, the chains are loosely packed,¹⁶ which suggests that chains are mobile in the hexagonal phase; consequently the hexagonal phase is often referred to as "the mobile phase".

The quantitative study on the growth mechanism of an isolated extended chain single crystal (ECSC), however, has not been carried out due to technical difficulties in observing the crystal growth rate under isobaric conditions at elevated pressure (P) which is important for the study of the growth mechanism. We showed that at the appropriate high pressure crystallization at low degree of supercooling (ΔT) of PE gives an isolated ECSC,³ as suggested by Bassett.¹³ We successfully observed the lateral growth rate (V) of an isolated ECSC by means of optical microscopy under isobaric conditions by constructing a new high pressure cell.¹⁸

We showed that ECSCs display some specific lateral habits and that the lateral growth rate (V) obeys the experimental relation

$$V = A \exp(-B/\Delta T) \quad (4)$$

where A and B are constants.¹⁸ These facts led to the conclusion that the lateral growth of ECSCs is nucleation controlled.¹⁹

We also found recently that the equilibrium triple point pressure is about 0.5 GPa. Therefore ECCs crystallized below the triple point pressure are formed in the metastable hexagonal phase. We discussed in detail the important role of the mobile hexagonal phase in polymer crystallization.²⁰

On the basis of these experimental results including those by Wunderlich, Bassett, Yamamoto, and us, we proposed a new kinetic theory named "chain sliding diffusion theory".²¹ The theory showed that the origin of ECCs and FCCs is related to the respective ease and difficulty of chain sliding diffusion within the nucleus and/or crystals. The concept of sliding diffusion along the chain axis reflects the topological nature of long chain molecules, which is quite different from that in atomic systems and systems of low molecular weight molecules. The theory itself succeeded to explain the observed ΔT dependence of V for an ECSC of PE.²²

The theory presented a new concept of the lamellar thickening growth of a single crystal (i.e., the primary crystallization). It successfully showed that the lamellar thickening growth rate (U) is large when polymers crystallize into the mobile phase where sliding diffusion is distinguishable, which will give formation of an ECSC, whereas the U is small when polymers crystallize into the immobile phase such as the orthorhombic phase where sliding diffusion is low, which will give formation of a folded chain single crystal.

Thus the theory predicted that all polymers which crystallize from the melt into the mobile phase will form ECCs, while polymers which crystallize into the more ordered and less mobile phase will form FCCs. The prediction has recently been confirmed on several polymers, in addition to PE,²⁰ namely in poly(chlorot-

trifluoroethylene) (PCTFE)²³, poly(*trans*-1,4-butadiene) (PT1,4BD),²⁰ and vinylidene fluoride/trifluoroethylene copolymers (P(VDF/TrFE)).²⁴

The purpose of the present paper is to show direct experimental evidence of the new crystallization mechanism of the "lamellar thickening growth" for an ECSC, i.e., primary crystallization, already briefly mentioned in a previous paper,²⁵ including direct evidence that an ECSC is formed from an FCC, and for the first time to measure the lamellar thickening rate (U) by two new methods developed for the purpose. Thus the prediction by the chain sliding diffusion theory will be confirmed by showing the important role of the lamellar thickening growth for the origin of an ECSC. The difference in the temperature dependence between U and W , corresponding to the primary and the secondary crystallization processes, respectively, will be also briefly discussed.

The present paper is the first in a series of two on "lamellar thickening growth" to be referred to as parts 1 and 2, respectively. In part 2 we shall report on the ΔT dependence of the U .

2. Experimental Section

The material of this study was highly fractionated polyethylene (PE) (NIST, SRM1483, $M_w = 32 \times 10^3$, $M_w/M_n = 1.11$). PE was crystallized under high pressure from the melt into the hexagonal crystals. A specially designed high pressure cell with a couple of diamond windows was used to observe crystallization behavior and structure by polarizing optical microscopy and by X-ray methods.²⁰ The pressure (P) range of this study was $P = 0.3$ – 0.5 GPa. The range of ΔT was 2–10 K. Samples were pressure quenched at a stage where isolated single crystals were formed (see Figure 1). These quenched samples were then etched by permanganic acid using Bassett's method,²⁶ and replicas were prepared in order to observe the morphologies by transmission electron microscopy (TEM). The detail of the experimental procedure were given in the previous paper.²⁰

3. Tapered Shape of an ECSC

3.1. Optical Microscopy. Figure 1 shows typical light optical images of extended chain single crystals observed by polarizing optical microscopy. Leaf- or cigarlike shapes are seen. Figure 1 shows ECSCs growing at 0.4 and 0.5 GPa. Figure 1a,b is below and Figure 1c is at the triple point pressure ($P_{\text{tri}} = 0.5$ GPa),²⁷ respectively. Figure 1a,b displays growing ECSCs at different ΔT s; 2.6 and 7.0 K, respectively. It is seen from Figure 1 that the overall light optical appearance of the crystals is not basically affected by pressure and ΔT , as mentioned in the previous paper.²⁰

3.2. Tapered Shape Observed by TEM. Figure 2 shows typical transmission electron micrographs of "edge-on" cross sections of isolated extended chain single crystals (ECSCs) observed on the etched surface of PE. Each crystal in Figure 2a, 2b, and 2c corresponds to the one indicated by an arrow in the corresponding light optical image of Figure 1a, 1b, and 1c, respectively. All cross sections have a straight "tapered shape" (or wedge shape) (Figure 3), as shown by Bassett.¹⁴ Some notes on the straight tapered shape are given in the Appendix. It will be shown in section 4 that the straight taper is evidence of linear increase of lamellar thickness with time.

The lamellar thickness (l) was very large, a few (or several) microns, at the center, while it was very small, only a few or several tens nanometers, at the tip of the taper which corresponds to the growth front. They are denoted as l_{max} and l_{tip} , respectively. In this study, the extended chain length of this sample (l_e) was about 0.3

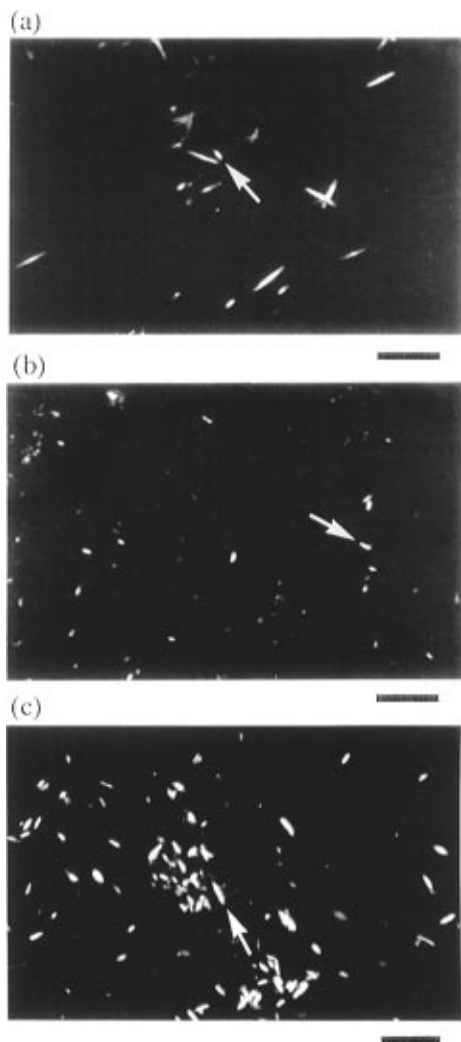


Figure 1. Typical polarized optical micrographs of ECSCs of PE under high pressure. Arrows show leaflike or cigar shapes. (a) $P = 0.4$ GPa and $\Delta T = 2.6$ K. (b) $P = 0.4$ GPa and $\Delta T = 7.0$ K. (c) $P = 0.5$ GPa and $\Delta T = 4.3$ K. Scale bar = $50 \mu\text{m}$.

μm . Another characteristic parameter of the tapered shape is "taper angle" (ϕ) defined in Figure 3.

As l_{max} is of the order of thickness of ECCs, while l_{tip} is that of FCCs after Wunderlich's definition,³ it can be considered that one single crystal shows continuous change in morphology from FCC to ECC within itself. Therefore there is no distinct difference between FCC and ECC, just as predicted by the chain sliding diffusion theory.²¹ To summarize

$$l_{\text{max}} = \text{a few } \mu\text{m} \quad \text{ECC at the center}$$

$$l_{\text{tip}} = \text{a few or several tens nm} \\ \text{FCC at the growth front} \quad (5)$$

for a "large" ECSC. Here by "large" ECSC we mean lateral length (a) much larger than a few tens microns.

Striations are clearly seen on the cross-sectional image implying that the molecular chains must be arranged parallel to these striations, which in turn are parallel to the short axis of the tapering lamellae.

3.3. ΔT Pressure, and Growth Dependence of the Tapered Shape. Figure 2 shows that the cross sections of samples crystallized at different ΔT or P represented closely similar straight linear tapered shapes. Therefore it is concluded that the tapered shape does not show significant ΔT or P dependence at least within the range observed in this study.

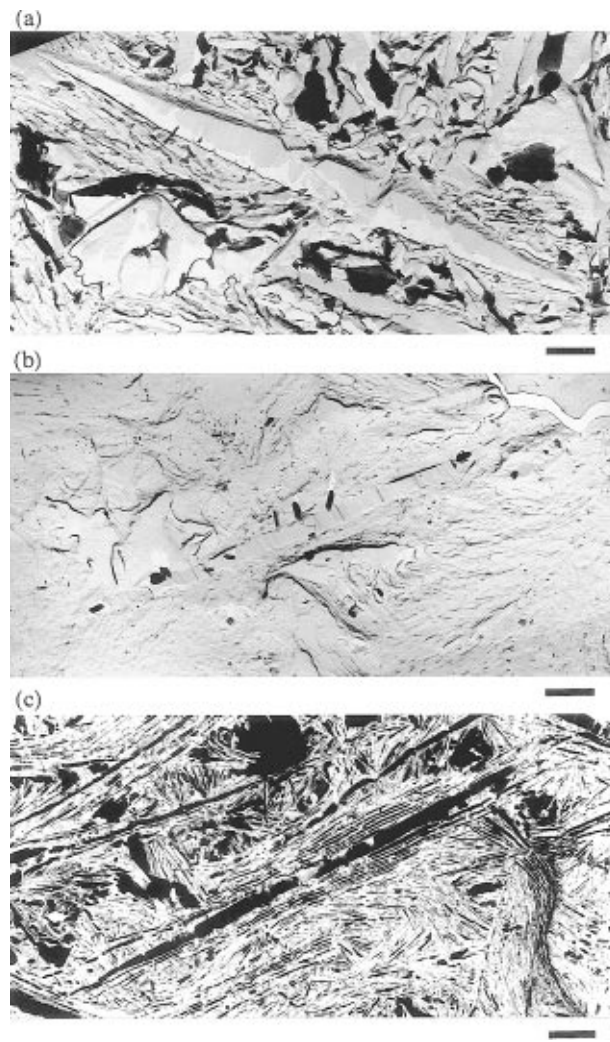


Figure 2. Typical transmission electron micrographs showing the linear tapered cross section of an isolated ECSC. (a), (b), and (c) correspond to those shown in Figure 1, respectively. Scale bar = $1 \mu\text{m}$.

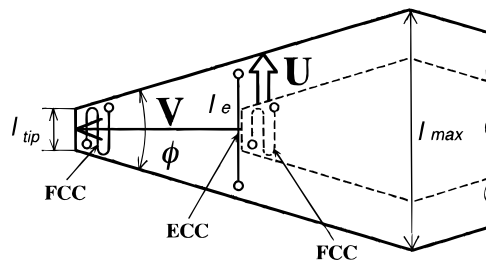


Figure 3. Schematic cross-sectional view near the tip (growth front) of an ECSC, showing tapered shape. l_{tip} , l_{max} , and ϕ indicate the lamellar thickness at the tip and the center and the taper angle, respectively. V and U show lateral growth rate and lamellar thickening rate, respectively.

It should be also stressed that similar tapered shapes are observed on various size of ECSCs seen within the same sample. The difference in size indicates the difference in crystallization time; i.e., a bigger crystal corresponds to a longer crystallization time. Figure 4 shows the size dependence (i.e., growth time dependence) of the tapered shape which is characterized by two parameters l_{tip} and ϕ . It is apparent that neither l_{tip} nor ϕ changes with size, i.e.,

$$l_{\text{tip}} \approx \text{constant} \quad (6a)$$

$$\phi \approx \text{constant} \quad (6b)$$

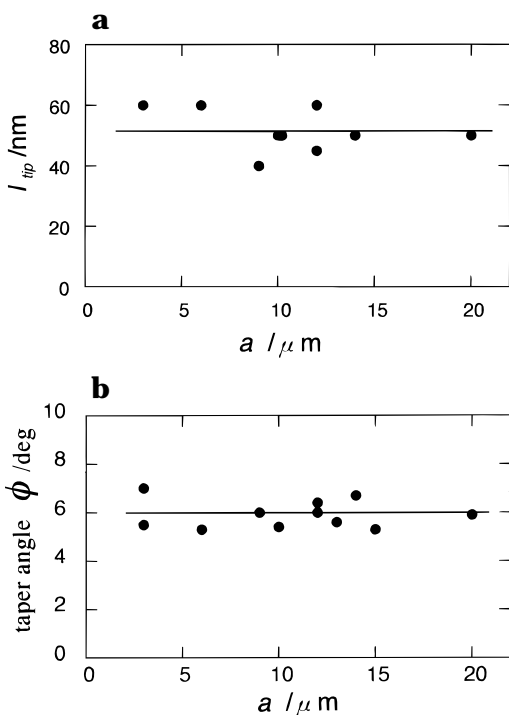


Figure 4. Plots of (a) l_{tip} against a and (b) ϕ against a , showing that they are constants.

Therefore we have the important conclusion that the same tapered shape is maintained during the growth of an ECSC, hence that the crystal is growing with constant shape.

Thus the straight tapered shape is the most characteristic morphology of an isolated ECSC as long as it is in isolation. It will be shown in section 5 that from the straight tapered shape the lamellar thickening growth rate can be estimated. The origin of the straight tapered shape will be explained theoretically in part 2 of this series. (This situation will change once the lamellae impinge leading to a parallel stack of layers.)

3.4. The Shape of an Isolated ECSC. As to the shape of a "flat-on" ECSC (this means the top view of a lamellar crystal), we shall assume here the circular shape as has been reported for ECSCs crystallized below 0.3 GPa (far from P_{tri}) by Bassett²⁸ or by ourselves in Figure 7 of ref 20. It is not definite at present whether the shape of an ECSC crystallized above 0.4 GPa (close to P_{tri}) is circular or not, because no ECSC crystallized above 0.4 GPa could be successfully extracted at least to our knowledge. The flat-on view shape has been studied using an improved extraction method based on that developed by Bassett et al.²⁶ Unfortunately the extraction of ECSC becomes more difficult for samples crystallized at increasing pressure, especially close to and above the P_{tri} .²⁹

The combination of the straight tapered shape and the circular shape assumed by a flat-on viewed ECSC gives a schematic perspective of an ECSC as shown in Figure 5. We mention only briefly here that the straight tapered shape is seen when the cross section passes through the center of the circular disk, while a round tapered shape is expected when it does not pass through the center. This point will be discussed in more detail in the Appendix.

4. Lamellar Thickening Growth

4.1. Thickening Growth Suggested by the Tapered Shape. Figure 5 illustrates the growth of a small ECSC into a large one. In Figure 3 the same is

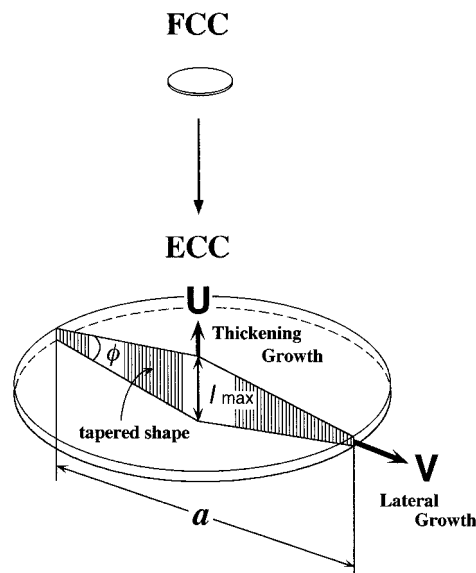


Figure 5. Schematic perspective of an ECSC showing two different growth mechanisms, lamellar thickening growth and lateral growth.

shown schematically in terms of changes of chain configuration in a cross-sectional view near the growth front. The chains are initially folded behind the growth front of a small crystal indicated by dotted lines in Figure 3. When the small crystal grows into larger one as indicated by the smooth lines, the thickness of the "old" growth front increases beyond the extended chain length. Consequently this indicates that FCC changes into ECC at that locality of the "old" growth front in Figure 3. At the same time the growth front advances perpendicular to the chain axis.

All the above indicates that a single crystal grows simultaneously in two directions; one is nearly parallel and the other nearly normal to the chain axis. The former indicates a new growth mechanism of polymer crystallization which we shall term the "lamellar thickening growth", whereas the latter corresponds to the well-known lateral growth. Here we shall denote the lamellar thickening growth rate by the symbol U . (The vector \mathbf{U} is defined to be parallel to the chain axis which is not normal to the end surface. This is different from the usual definition of the normal growth rate of a crystal face as a vector perpendicular to crystal surface.) The vector \mathbf{U} is shown in both Figures 3 and 5. The correspondence of the tapered shape of an ECSC to the thickening was first suggested quantitatively by Hodge and Bassett.¹⁴

4.2. Direct Evidence That ECC is Formed from FCC via Thickening Growth. Direct evidence that ECC is formed from FCC has been obtained for the first time, as is shown in Figure 6. Figure 6 is a succession of typical transmission electron micrographs of isolated single crystals seen in the same sample in the order of increasing lateral size a . It was shown in section 3.3 that a larger crystal arises after longer crystallization time (Δt). (For the definition of Δt see section 5.2 and Figure 7a). Therefore Figure 6 is a representation of the growing process for an ECSC with increasing Δt .

It is apparent from Figure 6 that the maximum lamellar thickness (l_{max}) at the center is only 0.15 μm for a small single crystal growing for short Δt , while it increases up to a few microns for a large single crystal after long Δt . It is obvious that the former is thinner than the extended chain length, $l_e = 0.3 \mu\text{m}$, whereas the latter exceeds the l_e . Consequently the small crystal

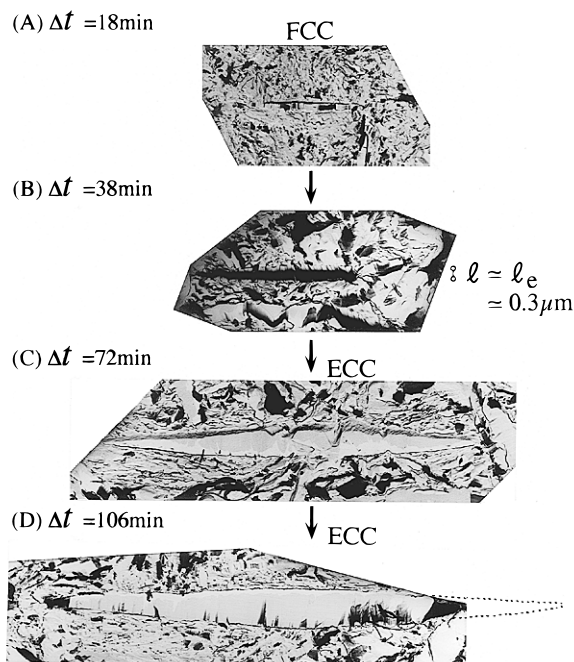


Figure 6. Transmission electron micrographs showing evidence that the ECC formed from FCC. $p = 0.4$ GPa, $\Delta T = 2.6$ K. Scale bar = $1 \mu\text{m}$. Δt is crystallization time and l_e is the length of an extended chain.

in Figure 6a must be a folded chain single crystal (FCSC), while the large crystals in Figure 6c,d must be ECSCs.

It is therefore concluded that an ECSC is generated from an FCC and grows to an ECC through coupling of the newly recognized lamellar thickening growth and the long familiar lateral growth. Thus there appears to be no significant gap between the formation of an FCC and an ECC; i.e., the morphological change from an FCC to an ECC is a continuous process.

5. Lamellar Thickening Growth Rate (U)

5.1. Definition of U . The lamellar thickness of an ECSC is a function of time (t). Hence the thickening growth rate U can be defined as

$$U = (1/2)(dI/dt) \quad (7)$$

If we assume that U is constant throughout the growth of the crystal (which will be confirmed later in this paper), I will be given by

$$I = I^* + 2Ut \quad (8)$$

where I^* is thickness of the critical nucleus.

If we could observe the increase of I with t , U could be obtained using eq 7. However, it is difficult at present to carry out such an observation directly during growth. I can be measured only by TEM, which means only after quenching. Therefore it is necessary to find some special methods to measure U , such as is essentially equivalent to following changes in I directly (eqs 7 and 8).

Here we shall propose two different methods to measure U . We shall call them "direct method" and indirect method (or "mapping method") to be described below. (The latter was already mentioned in ref 20).

5.2. "Direct Method" To Measure U . **a. Theory.** It was shown in section 4.2 that I_{max} increases with increase of Δt . Thus we can define a special U , U_d , by

$$U_d = (1/2)(dI_{\text{max}}/d\Delta t) \quad (9)$$

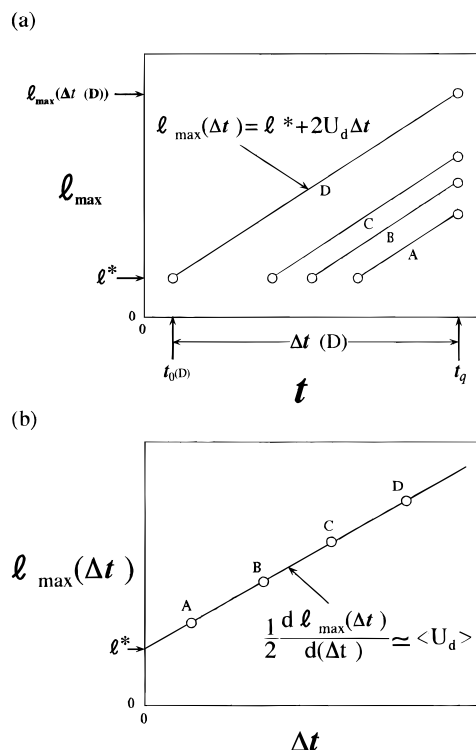


Figure 7. Principle of the direct method. (a) The lamellar thickness (I_{max}) against time (t) of single crystals, A, B, C, and D generated at different occasion. Δt is crystallization time. (b) Change of I_{max} with Δt .

which is equivalent to eq 7. If we assume that U_d is constant, we have

$$I_{\text{max}}(\Delta t) = I^* + 2U_d\Delta t \quad (10)$$

This is equivalent to eq 8. Figure 7a illustrates the change of I_{max} with Δt as given by eq 10.

Here Δt is defined as the time interval between the time of birth of each ECSC (t_0) and the time at quenching (t_q), as is illustrated in Figure 7a, i.e.,

$$\Delta t \equiv t_q - t_0 \quad (11)$$

Figure 7a schematically illustrates that the ECSCs A, B, C, and D arose at different t_0 but quenched at the same t_q ; hence $I_{\text{max}}(\Delta t)$ at $t = t_q$ corresponds to different Δt values. The $I_{\text{max}}(\Delta t)$ values are plotted against Δt schematically in Figure 7b, which should give a straight line if the assumption that $U = \text{constant}$ is correct.

The gradient of the line gives a kind of U which is equivalent to an average of U_d of ECSCs A, B, C, and D. We shall denote it $\langle U_d \rangle$. This method to measure U we shall name the "direct method". In this method it is not necessary to know the value of I^* (which is of course difficult to obtain).

b. Results. The growth behavior of ECSCs was observed directly by optical microscopy and recorded by a video system. In this way Δt of ECSCs defined by eq 11 could be directly measured. For each selected ECSC, observed by optical microscopy, there could be obtained a directly corresponding electron micrograph as shown in Figures 1 and 2. Thus both Δt and I_{max} for each ECSC could be measured directly.

Figure 8 shows the observed I_{max} values plotted against Δt . As seen, the I_{max} increased linearly with increasing Δt . From the gradient of the line we obtained $\langle U_d \rangle = 0.20$ nm/s, providing for the first time a quantitative measure of U . This confirmed that the lamellar thickening growth is a steady growth process, that the

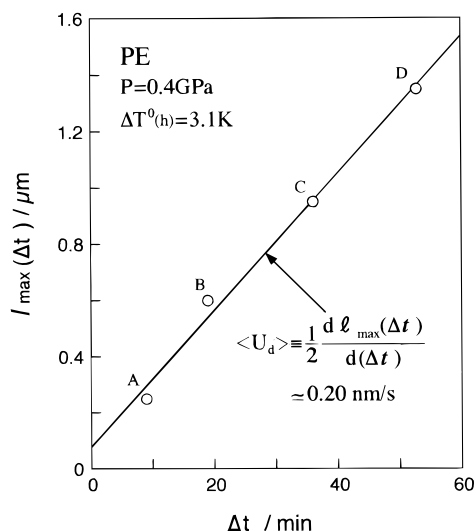


Figure 8. Plot of the maximum lamellar thickness (l_{\max}) against Δt .

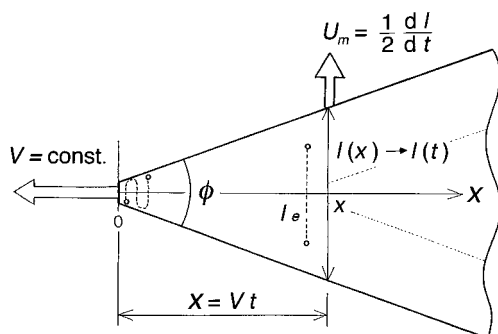


Figure 9. Schematic cross-sectional view of an ECSC. x , $l(x)$, and $l(t)$ are explained in the text.

assumption of $U = \text{constant}$ is correct and that an FCSC grows continuously into an ECSC.

5.3. Indirect Method ("Mapping Method") To Obtain U . **a. Theory.** To explain the "mapping method" we refer to an illustration of the straight tapered crystal such as Figure 9. We define the x -axis as the normal to the lateral face at the tip (i.e., lateral growth front) of an ECSC. Taking the origin of the x -axis at the tip itself, the l of an isolated ECSC can be mapped as a function of x :

$$l = l(x) \quad (12)$$

As V is also normal to the lateral face at the tip side surface,

$$x = Vt \quad (13)$$

where t represents the time interval required for the growth front to cover the distance x . Hence,

$$t = x/V \quad (14)$$

Combination of eqs 12 and 14 gives

$$l = l(t) \quad (15)$$

Equation 15 is equivalent to eq 8; hence U can be obtained through eq 7. Thus we can obtain U by combining $l(x)$ (as mapped) and V . We denote U thus obtained through the above defined "mapping method", as U_m . In fact, in the case of a straight tapered crystal U_m is given by the slope, i.e., $1/2\phi$, directly.

The mapping and the direct methods will be compared further in part 2 of this series.

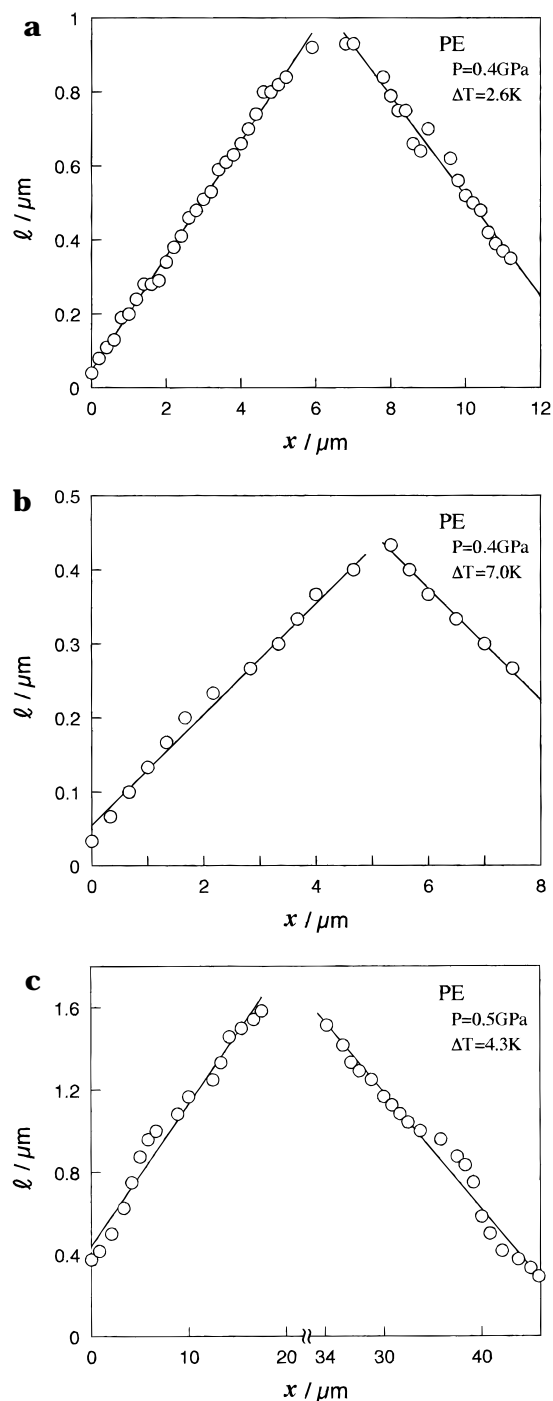


Figure 10. Lamellar thickness (l) as a function of distance (x) of an ECSC. (a), (b), and (c) correspond to those shown in Figure 2, respectively.

b. Results. Typical "mapped" lamellar thickness as a function of x , $l(x)$, is shown in Figure 10. The (a), (b), and (c) in Figure 10 were obtained on the ECSCs which correspond to (a), (b), and (c) in both Figures 1 and 2. In all cases l vs x is a straight line, corresponding to the straight tapered shape of the cross section of an the ECSC, as seen directly from the electron micrograph.

Figure 11 shows a typical example of the observed lateral length a as a function of t corresponding to Figure 10a, from which the lateral growth V was obtained. Combination of the mapped $l(x)$ and V then gives the $l(t)$ through eq 14, as plotted in Figure 12, corresponding to the respective l vs x plots of Figure 10.

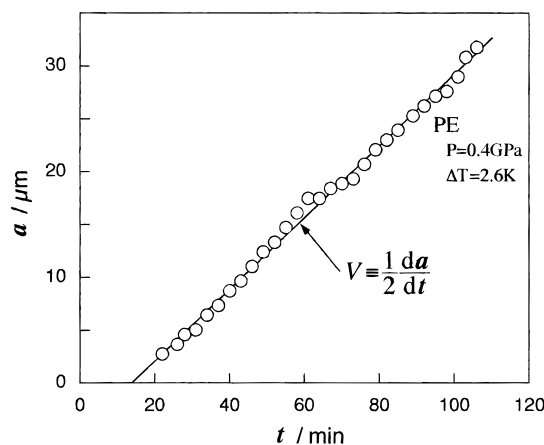


Figure 11. Lateral length (a) as a function of time (t).

It is apparent from Figure 12 that l increases linearly with time, indicating steady lamellar thickening growth. The gradient of the straight lines in Figure 12 gives the values of U_m by eq 7. The values of U_m are displayed in Figure 12.

5.3. ΔT Dependence of U . It is shown in Figure 12a,b that U at $\Delta T = 2.6$ K is smaller than that at $\Delta T = 7.0$ K, which indicates that U increases with increasing ΔT , i.e.,

$$dU/d\Delta T > 0 \quad (16)$$

The positive ΔT dependence of U is opposite that of the lamellar thickening rate (W) of the stacked lamellar system shown in eq 3. The quantitative ΔT dependence of U will be reported in part 2 of this series.

6. Discussion

6.1. Differences between Lamellar Thickening Growth and the Conventional Lamellar Thickening. We have shown in section 5 that for an isolated ECSC the thickening growth rate (U) is constant and that U increases with increasing ΔT . This is quite different from a viewpoint of the thickening rate (W) which is not constant but decreases with time and also with increasing ΔT . These remarkable differences suggest that the origin and mechanism of lamellar thickening growth of an isolated lamella and that of lamellar thickening of stacked lamellae must be quite different. We shall show in part 2 of this series that the difference is due to that between primary and secondary crystallization. The former is a crystallization process of a single lamella within the melt where new chains can be supplied easily from the melt, whereas the latter is a recrystallization process of the stacked lamellae where no chains can be supplied and each lamella will be healed into a thicker lamella due to thermodynamic driving force.

6.2. Origin of ECC and FCC. We have also shown in section 5 that $U = 0.2$ nm/s and $V = 2.0$ nm/s at $P = 0.4$ GPa and $\Delta T = 2.6$ K. Thus although the value of U is smaller than V , U is still significant and determines the thickness and, in conjunction with V , the slope of an ECSC. This confirms a prediction of the chain sliding diffusion theory presented by one of us (M.H.), namely, that when U is not negligible compared to the lateral growth rate (V), a polymer single crystal will become an ECSC. The theory also predicts that when U does become negligible compared to V , the final

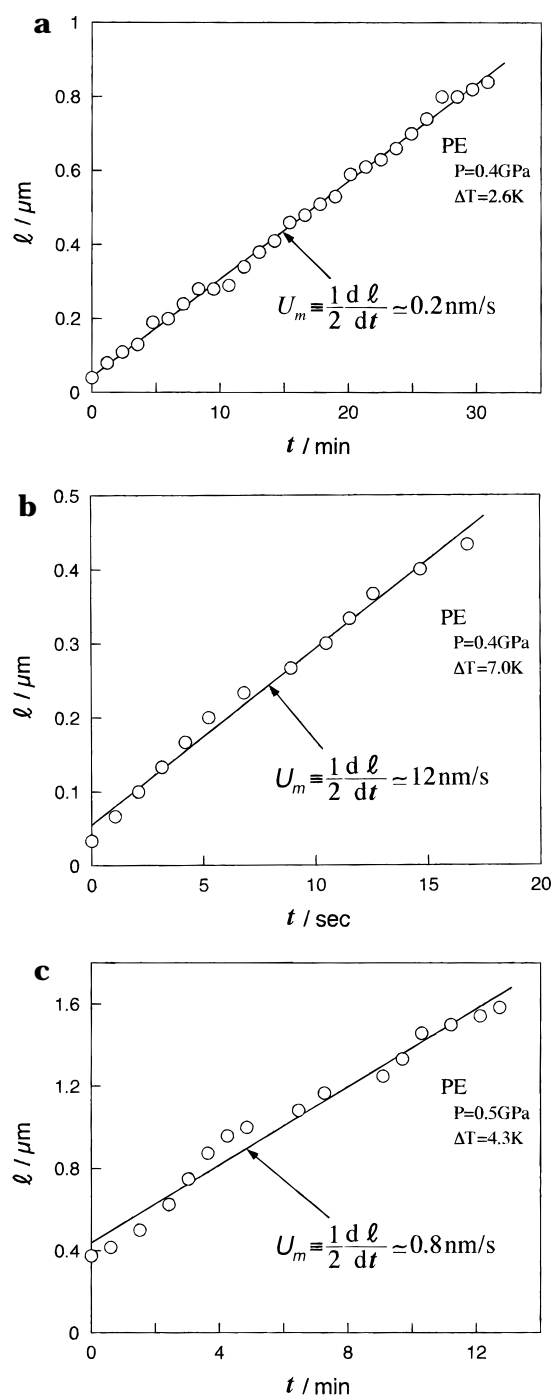


Figure 12. Lamellar thickness (l) as a function of time (t) of an ECSC. (a), (b), and (c) correspond to those shown in Figure 2, respectively.

crystal will have the characteristics of FCC. Further support for this assertion will be reported in near future.

Thus we could conclude that the origin of ECC and FCC is related to the ratio of U/V , namely, when U/V is finite, say within an order of magnitude of unity, the crystal will have the character of ECC, while when U/V is very small, say close to zero, it will fall in the category of FCC.

7. Conclusion

It is found that an extended chain single crystal (ECSC) of PE is formed from a folded chain single crystal through the coupling of the newly found lamellar thickening growth and the familiar lateral growth.

The lamellar thickness (l) increases linearly with time from which the lamellar thickening growth rate (U) can

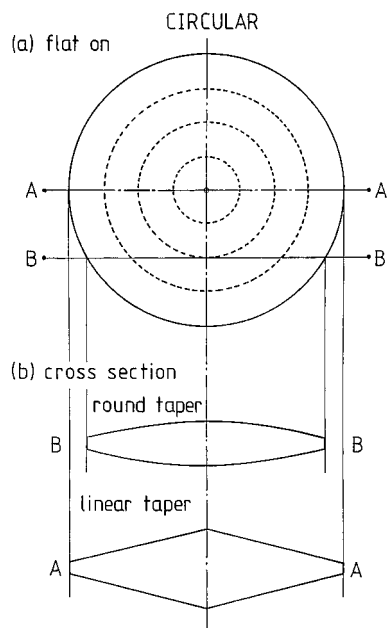


Figure 13. Illustration of (a) flat-on shape and (b) cross section of an ECSC which is assumed to have circular shape. AA and BB indicate the positions of sections.

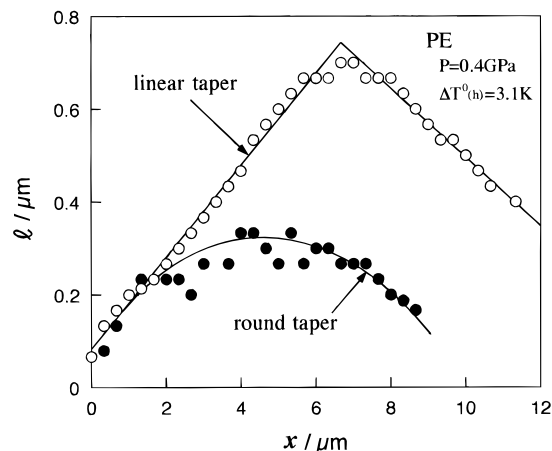


Figure 14. Typical plots of l against x .

be estimated by the definition $U = (dl/dt)/2$, a quantity directly reflected to the external shape, namely, the taper angled crystal when still in isolation.

The lamellar thickening growth rate was determined for the first time through two new methods, termed "direct" and "mapping" methods.

At a given undercooling (ΔT) the ratio of thickening growth (U) and lateral growth (V) is a constant with $U/V < 1$ with the consequence that crystals are growing at a constant shape: this has further important implications for the mechanism of crystal growth.

Acknowledgment. The authors are grateful to Prof. A. Toda of Hiroshima University and Prof. Ohigashi of Yamagata University for their helpful discussions. This work was partly supported by a Grant-in-Aid for Scientific Research (B) No. 7455386 and that of (C) No. 6651038, that on Priority Areas "Crystal Growth Mechanism in Atomic Scale", No. 04227105, that for Developmental Scientific Research (B), No. 04555212 and that for Cooperative Research (A), "Polymer Crystallization and Texture Formation Mechanism", No. 04302055, and International Joint Research Grant, NEDO, 1996–1998.

Appendix. Notes on the Tapered Shape of Cross Section of an ECSC

The tapered shape of the cross-sectional view of an ECSC was shown in section 3.2. The straight taper will be expected only for the case that the cross section passes through the center of an ECSC, while in other cases, a round shape is expected, as shown in Figure 13. Here the circular shape is assumed for the shape of a flat-on ECSC. Figure 14 shows the typical linear tapered shape and the round shape observed in the same sample. Therefore all observations in this work were carefully carried out by selecting the straight tapered shape.

The straight taper was seen on an ECSC which has transformed from the hexagonal to orthorhombic forms during the pressure quenching process. It is well-known that a single crystal in hexagonal form will be divided into domains with the transition to the orthorhombic form and that chains in one domain are usually differently inclined from those of neighboring domains. If the inclination angle is large as in the case of FCC of PE, where it reaches a few tens or several tens degrees, the dividing into domains causes misfit with each other and the linear taper cannot be observed. Therefore the observed result of the linear taper shape suggests that the inclination angle is not so large in the case of an ECSC lamella.

References and Notes

- (1) Keller, A. *Philos. Mag.* **1957**, *2*, 1171.
- (2) Wunderlich, B.; Arakawa, T. *J. Polym. Sci.* **1964**, *2*, 3697.
- (3) Wunderlich, B. *Macromolecular Physics*; Academic Press: New York, 1973; Vol. 1.
- (4) Statton, W. O.; Geil, P. H. *J. Appl. Polym. Sci.* **1960**, *3*, 357.
- (5) Fischer, E. W.; Schmidt, G. F. *Angew. Chem.* **1962**, *74*, 551.
- (6) Anderson, F. R. *J. Appl. Phys.* **1964**, *35*, 64.
- (7) Peterlin, A. *Macromol. Chem.* **1964**, *74*, 107.
- (8) Hirai, N.; Mituhata, T.; Yamashita, Y. *Kobunshi-kagaku* **1961**, *18*, 33.
- (9) Calvert, P. D.; Uhlmann, D. R. *J. Polym. Sci., A2* **1972**, *10*, 1811.
- (10) Yasuniwa, M.; Enoshita, R.; Takemura, T. *Jpn. J. Appl. Phys.* **1976**, *15*, 1421.
- (11) Wunderlich, B.; Melillo, L. *Makromol. Chem.* **1968**, *118*, 250.
- (12) Nash, H. A.; Grossman, S. R.; Bassett, D. C. *Nature* **1968**, *219*, 368.
- (13) Bassett, D. C.; Turner, B. *Philos. Mag.* **1974**, *29*, 285.
- (14) Rees, D. V.; Bassett, D. C. *J. Polym. Sci.* **1971**, *9*, 385.
- (15) Bassett, D. C.; Block, S.; Piermarini, G. J. *J. Appl. Phys.* **1974**, *45*, 4146.
- (16) Yamamoto, T.; Miyaji, H.; Asai, K. *J. Appl. Phys.* **1977**, *16*, 1891.
- (17) Hikosaka, M.; Tamaki, S. *J. Phys. Soc. Jpn.* **1981**, *50*, 638.
- (18) Hikosaka, M.; Seto, T. *Jpn. J. Appl. Phys.* **1982**, *21*, L332.
- (19) Hikosaka, M.; Seto, T. *Jpn. J. Appl. Phys.* **1984**, *23*, 956.
- (20) Hikosaka, M.; Rastogi, S.; Keller, A.; Kawabata, H. *J. Macromol. Sci. Phys.* **1992**, *B31*, 87.
- (21) Hikosaka, M. *Polymer* **1987**, *28*, 1257; *Polymer* **1990**, *31*, 4.
- (22) Hikosaka, M.; Koizumi, T.; Shioda, S.; Seto, T. First AIM conference on advanced Topics in Polymer Science; *Europhys. Conf. Abstr.* **1988**, *12D*, 76.
- (23) Hikosaka, M.; Kasahara, T.; Rastogi, S.; Keller, A.; Kawabata, H.; Kanazawa, T. *Polym. Prepr. (Am. Chem. Soc., Div. Polym. Chem.)* **1989**, *30*, 307.
- (24) Hikosaka, M.; Sakurai, K.; Ohigashi, H.; Koizumi, T. *Jpn. J. Appl. Phys.* **1993**, *32*, 2029.
- (25) Hikosaka, M.; Amano, K.; Rastogi, S.; Keller, A. *Crystallization of Polymers*; NATO ASI Series; Kluwer Academic Press: London, 1993; p 331.
- (26) Olley, R. H.; Hodge, A. M.; Bassett, D. C. *J. Polym. Sci. Polym. Phys. Ed.* **1979**, *17*, 627.
- (27) Hikosaka, M.; Tukijima, K.; Rastogi, S.; Keller, A. *Polymer* **1992**, *33*, 2502.
- (28) DiCorleto, J. A.; Bassett, D. C. *Polymer* **1990**, *31*, 1971.
- (29) Okada, H.; Hikosaka, M.; Toda, A. *Polym. Prepr. Jpn.* **1994**, *43*, 3309.